Research Article

Analysis of the Influence of Arc Volt-Ampere Characteristics on Various Loads and Methods for Detecting Series Arc Faults

Dzhavat Dzhavatov [1,2], Alexander Uryupin[3,*], Sergei Kiselev[4] and Aleksandr Beloglazov[5]

[1]*Institute for Geothermal Research and Renewable Energy – Branch of the Federal State Budgetary Institution of Science United Institute of High Temperatures of the Russian Academy of Sciences, Makhachkala, Russian Federation*
[2]*Dagestan State University, Makhachkala, Russian Federation*
[3]*Russian University of Transport (MIIT), Moscow, Russian Federation*
[4]*Russian Technological University, Moscow, Russian Federation*
[5]*Tomsk Polytechnic University ELTI, Tomsk, Russian Federation*

_____

Abstract

The problem of accurate detection of series arc faults in consumer networks is still relevant today. Despite many modern methods of detection and protection, every year there are many residential fires caused by arc faults. The purpose of this study is to perform a detailed analysis of Alternating Current (AC) and voltage variations due to arc faults based on the volt-ampere characteristics and develop a more accurate detection method of series arc faults. The peculiarities of changes in current and voltage signals of the circuit at purely resistive, diode rectifier with capacitor and inductive filter, resistive-inductive types of load were analyzed and determined. A method for detecting serial arc faults based on an algorithm for sequential detection of current signal features has been proposed. It was found that network trippings at arc faults comply with the standards of State Standard of the Soviet Union (GOST) (rus) (SUST) (eng) IEC 62606-2016 for user electrical appliances (national standards of the Russian Federation harmonized with International Electrotechnical Commission (IEC) standards. The obtained theoretical and experimental results of this study can be used to develop an effective methodology for recognizing arc faults in the consumer network.

Keywords: AC, Arc fault, Series arc faults, Volt-ampere characteristic, Protection, Voltage variation

_____

1. Introduction

Arc faults are among the main causes of fires in factories and residential buildings. According to statistics from the All-Russian Research Institute of Fire Defense (ARRIFD) of the Russian Federation (RF) Ministry of Emergency Situations [1], in 2020, 51,930 fires occurred from electrical products, which was 11.82% of the total number of fires in the country. The same ratio is typical of many industrialized countries in Europe, where an average of 24.39% of fires are caused by improper use of electrical appliances, as well as by improper actions of personnel or aging network equipment [2].

In the majority of cases, the causes of fires from electrical equipment are deficiencies in design and manufacturing, non-compliance with international standards of the materials and components used, imperfect fire safety requirements, low level of operation and Serial Arc Faults (SAF) [1]. One way to reduce the risks of SAF is to focus on protecting consumer and manufacturing networks from this phenomenon and adopting appropriate product standards. For example, many countries have formulated standards for electrical systems such as UL1699 (the USA) [3], IEC62606 (International Electrotechnical Commission) [4], GB14287.4 and GB/T31143 (China) [5], [6].

Overcurrent and short-circuit in the consumer electrical network can be detected by the circuit breaker as well as by the voltage control loop based on the integrated circuitry. The

voltage control loop is used as an approach to short-circuit protection with step-up converter to protect the DC bus, load and converter components against short-circuit current [7]. In the case of SAF, the circuit breaker may fail to trip, which can result in a fire that causes not only property damage, but also death and serious injury to people. This is because the RMS (Root Mean Square) value of the mains current at SAF is lower than the effective value at no SAF and lower than the overcurrent values for which the devices are designed [8]. Therefore, the main difficulty in arc fault protection is to accurately determine the SAF based on integrated short-circuit protection schemes.

1.1 SAF detection methods
In recent years, much research has been done on accurate SAF detection and modeling of this process. Arc fault detection methods are based on the detection of current and voltage deviations and their respective derivatives. When SAF occurs, depending on the load, the current signals have different frequency-time characteristics, where signal fluctuations increase and their periodicity is lost [9]. To distinguish signatures at SAF, current characteristics are divided into time and frequency domains. In the time domain, the rates of change in the effective value of current, pulse current, average current, and shoulder ratio are studied [10]. The pulse current can be seen as a special point in the current signal, and the random high-frequency component of the current signal makes the current signal unsteady. The rate of change of current increases and the shoulder coefficient decreases with increasing frequency [11]. When SAF occurs,

_____

the electrode or cable will volatilize due to the occurrence of an arc fault, resulting in incompatible current forms in different half-periods under arc fault conditions. To detect the SAF phenomenon, volt-ampere characteristics (VAC) are analyzed using various time domain algorithms, such as time domain analysis, broadband noise, and algebraic derivation [11-14].

Some nonlinear loads have arcing features in power systems, which include rectifiers (used in power supplies) and arcing devices such as fluorescents, electric welding machines, and arcing furnaces. Current in such systems is interrupted by switching action and contains frequency components that are multiples of the power system frequency. Nonlinear loads are inherent in changing the shape of the current voltage from sinusoidal to distorted waveforms, which creates harmonic currents and waveform distortions in addition to the original AC current. This is important in power systems that contain nonlinear loads, such as rectifiers, electric lighting forms, electric arc furnaces, and welding equipment. Line capacitor and conductor filters can prevent harmonic currents from entering the power system [10], [11], [15].

To reduce harmonic current in rectifiers with nonlinear loads, schemes of control algorithms with a predictive model based on a fixed switching frequency and dead time compensation are used [13]. The use of such a circuit provides dead time compensation to effectively suppress the effect of zero current compression, and the total harmonic current distortion is equal to the minimum value at different values of the dead time. Distortion of the voltage curve caused by the voltage curve distortion caused by the non-linear character of the Volt-Ampere Characteristic (VAC) of the arc, adversely affects the operation of all kinds of Electric Receivers (ER).

In the frequency domain, the harmonic component, odd and even harmonics are studied [15]. When SAF occurs, the shape of the current curve is distorted, which leads to the formation of harmonics, which have an inverse dependence on the current frequency. These characteristics are extracted in a constant frequency system, which cannot be applied to a variable frequency system. In the frequency domain, methods such as wavelet transform, Fourier transform, and Hilbert-Huang transform are used [14], [16], [17]. The wavelet transform method is characterized by the fact that wavelet packets are used to process the current waveform in the arc short-circuit, and then the characteristic parameters and frequency range of the current signal are extracted for detection [14]. In contrast to this method, the Fourier transform presents the signal and the amplitude value as the RMS value for each harmonic [16]. To decompose a complex signal at SAF, using the Hilbert-Huang transform for instantaneous frequency, one can extract the instantaneous amplitude value as an indicator of arc current [17]. However, for all of the above methods, it is necessary to set indicator thresholds, which may not be chosen correctly.

The method of sinusoidal forced current with mathematical models based on integral methods, which are widely applied to a large number of mathematical models for research of electric arc, can be used to improve the accuracy of determining the VAC [18]. The use of integral methods, as opposed to spectral methods, contributes to the reduction of errors in VAC measurement with high accuracy of parameter determination.

1.2 Modern machine learning-based methods of arc faults detection

Recently, a number of studies have used machine learning-based methods to detect arc faults and help classify the situation [19-23]. In [20], an optimized reference vector machine method was used to identify interference from power supply harmonics and nonlinear load noise to classify their features and detect SAF. For more accurate arc short-circuit recognition and phase selection, the reference vector machine method was optimized using grid search and particle swarm optimization algorithms [22]. Besides, deep learning neural networks also give good accuracy in classifying normal and arc current measurements [23]. However, methods based on machine learning require large amounts of high quality sampling data to achieve higher accuracy. Moreover, these methods only detect linear current and it is difficult to determine the type of load, which increases the difficulty of correctly detecting SAF. In order to improve energy efficiency in electrical networks, methods are used to accurately measure the power dissipated in active loads using a model of the electrical network and the frequency response of the current sensor to estimate the power indicators [21].

1.3 Problem statement
The purpose of this work was to study the effect of VAC of Arc Short-Circuit (ASC) on the variation of AC in a circuit under different load conditions. A circuit simulation is used as the basis, where the ASC can be represented as a dynamic nonlinear element. Based on the VAC analysis, a method was developed for the sequential detection of ASC in AC using algorithms for shoulder detection and current pulse fixation, detection of randomness in the form of VAC signals. The effectiveness of the method was checked on the basis of testing results in the study of different load types (fluorescent lamp, vacuum cleaner, and electric drill). The experimental results and theoretical VAC analysis provide a good basis for modeling and developing new techniques for detecting SAF in the consumer network.

2. Materials and Method

2.1 Methods for studying VAC of arc faults
The VAC of the alternating arc current is shown in Figure 1, where the arrow shows the direction of current change with voltage change in the case of a constant value of the distance between the electrodes (steady-state arc burning) [24]. As can be seen from the Figure, the arc resistance, which corresponds to the ratio U_{arc}/I_{arc}, is not constant and reaches a large value at the zero point, which leads to the arc extinction.
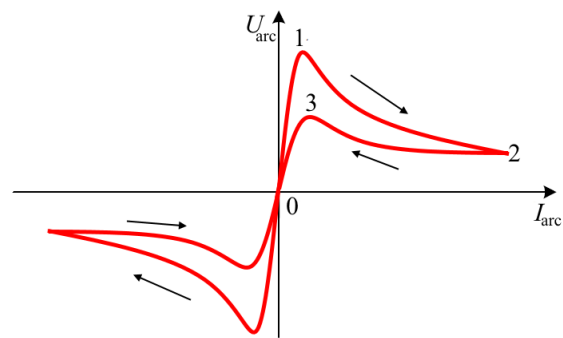

Fig. 1. VAC of the arc at AC

As can be seen from Figure 1, as the voltage increases U_{arc} to the arc ignition point (1), the current I_{arc} increases slightly and therefore the arc resistance remains quite large,

but gradually decreases. After reaching the ignition point, there is a sharp increase in current I_{arc} and voltage reduction U_{arc} to the next critical point (2), which is accompanied by a decrease in arc resistance [10]. After reaching point 2 there is a decrease in the current I_{arc} to point 3, but because of the thermal inertia of the electrode and the arc gas at the same current, the arc resistance will be less than in 1-2, which affects a lower voltage value U_{arc} in point 3.

At point 3, the arc is extinguished and a further decrease in current is accompanied by a decrease in voltage and an increase in resistance on the electrodes. During the reverse VAC similar processes occur (Figure 1). However, VAC of an AC arc are strongly related to the temperature of the arc, power supply voltage, and the electrode material [25], [26]. In addition, the composition of the electrode material may change after combustion, and some of the material may evaporate at high temperatures, resulting in changes in electrode spacing and, consequently, AC arcs may not coincide in different cycles.

2.2 SAF determination method and experimental setup
In accordance with the IEC 62606-2016 standard [27], a test bench was used for general requirements for arc fault detection devices under different types of loads, the electrical diagram of which is shown in Figure 2.
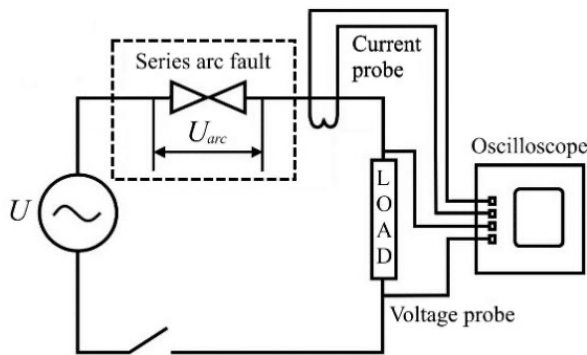

Fig. 2. Scheme of the bench for the study of SAF VAC at different load types in the AC circuit

A Rigol MSO5074 digital oscilloscope (sampling rate 250 kHz) was used to study and record VAC signals. A Testo 755-1 current tester was used to record current signals, and a Fluke T150 / 50 MHz tester was used to resolve voltage signals. The SAF generator consisted of two electrodes in the form of rods, one of which was carbon-graphite and was fixed on a shaft. The other rod of copper was driven by a motor which regulated the distance between the electrodes. The input voltage corresponded to 220 V with a frequency of 50 MHz. For adjusting the distance between the copper rod and the carbon rod to generate the arc, the input voltage was 220 V.

The AC arc fault detection algorithm is shown in Figure 3 and is based on the transient processes of ignition and extinguishment of the arc fault around zero crossing, which create a symmetrical energy profile. When this symmetrical energy profile is observed for a fixed number of cycles, an arc fault occurs.
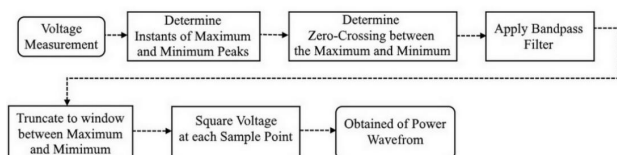

Fig. 3. Algorithm for obtaining the power of the voltage signal at each time instant

The SAF detection algorithm consists of the following sequential steps. The recorded signal data were pre-processed using the wavelet transforms in the Matlab program on the computer. This algorithm determines whether the number of SAF in a certain time corresponds to the conditions for starting protection according to IEC 62606-2016 standard [28], in which, if the current reaches 75 A within 0.5 s, and there are 12 half-periods of ASC, then the alarm and protection are triggered.

Step 1: Determining the half-period. The half-period of the AC source voltage was used as the unit of time to determine the presence of an arc fault, since it is almost independent of the load. The zero crossing point of the AC input voltage is used as the start of the external interrupt source. When SAF is detected in an identified time unit, the program determines that this time unit is the fault unit and a value of 1 is added to the number of arc events.

Step 2. Determine the phase relationship between the voltage and current of the power supply, and a preliminary estimate of the type of load, which are given by the waveforms under normal conditions.

Step 3. Shoulder detection on the current signal. In each identified ASC time unit, N fixed frequency current signals are detected. When the absolute value of the sample is below the set threshold (I_{max1}), and the absolute value of the difference between one sample point and the next sample point is below the following threshold (I_{max2}), then this sample point is evaluated as the current zero crossing point. The number of these points in each identified ASC time unit can be considered as the shoulder time.

Step 4. Pulsed current detection. The difference between each of the two adjacent current signals in one identified ASC time unit is calculated. This determines the rate of signal increase/decrease in that identified unit of time. If the increase/decrease of the current signal exceeds the threshold of 75 A, this detects the presence of pulse current. The number of pulse currents in each half-period is counted.

Step 5: Detecting randomness. The procedure for determining the randomness of the current waveform in the line is as follows. The absolute value of N current signals collected in each unit of time to identify an ASC fault is written as $i(t)_n$. For example, when at 220 V the value of current reaches 15 A (Figure 8) within a time interval of 0 to 0,6 s, the half-periods of the curves may constitute the optimum values of current and voltage. Adjacent values in the event of an arc may indicate a change in these parameters, which lend themselves to a change in the waveform of the half-periods with respect to adjacent time intervals. In this way a total count of the frequency-time relationship is carried out to determine Sn on the basis of the collected half-periods with each unit of time. The randomness of the corresponding sampling points of three neighboring blocks is calculated according to the equation (1):

$$S_n = (|i(t)_{n-1} - i(t)_n| + |i(t)_{n+1} - i(t)_n|) - |i(t)_{n+1} - i(t)_{n-1}|), m \geq 2 \tag{1}$$

Where S_n is a sum of all $i(t)$
n represents the unit number
t represents the sample point number within each unit, where $1<n<N$
In the study, the amplitude of the actual limits is 15 amperes at a threshold of 20 A at 220 V.
Then the S values of all N current signals are added

$$\delta = S_1 + S_2 + S_3 + \cdots S_n \qquad (2)$$

When no arc occurs the value of δ is at the minimum interval, when an arc occurs the value of δ increases and can reach the maximum value. If the value of δ represents a large defined threshold, it indicates that the time identification units are in a faulty state and makes it difficult to measure accurately.

3. Results and Discussion

3.1 VAC analysis for different types of loads on the network

A schematic representation of the waveform for current and voltage under normal condition with AC ASC is shown in Figure 4.
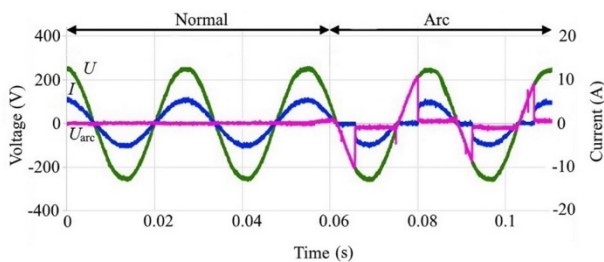

Fig. 4. Waveform representation for current and voltage during normal circuit connection and during ASC occurrence over time

As can be seen, there is a shoulder on the current curve and a sawtooth waveform for the voltage when the arc is generated. At the moment of reaching I zero the arc is extinguished and because of the high resistance at the ends of the electrodes a shoulder on the signal curve is observed I. At the same time U_{arc} is equal to the value of the voltage on the power supply U. When the arc ignition point is reached (point 1 in Figure 1), the voltage U_{arc} drops sharply and a sawtooth waveform is formed at the arc. In this case, the value of I increases sharply at the occurrence of SAF. That is, when a series arc occurs in an AC circuit, the linear current is very close to zero for a period near the natural zero crossing point. As can be seen from Figure 4, U_{arc} values may differ in different half-periods. This phenomenon is explained by the fact that in the case of ASC, the arc combustion is often accompanied by partial evaporation of the electrode material, which leads to dynamic changes in the arc gap distance, the composition of the surrounding gas and the arc temperature.

With a resistive type of load (ordinary resistor, incandescent lamp, fluorescent lamp) in the case of ASC, the waveform will change as shown in Figure 4, where the current waveform has shoulders. From the above analysis, it can be seen that in the case of a purely resistive load, SAF occur and the waveform has the following characteristics:

- the current is in phase with the source voltage;
- there are shoulders and sharp jumps in the value of the current strength after them, which is mainly determined on the basis of the values of the arc ignition voltage and the load resistance;
- after a sharp change, the current waveform corresponds to a sinusoidal one.

It should also be noted that when ASC occurs, the actual distance between the electrodes is not clearly defined, so the voltage is variable and the arc resistance is constantly changing, which leads to a random character of the current curve in different half periods.

For the case of a diode rectifier with a capacitor filter (switching power supply used in PCs, chargers, and LCD displays), the VAC of arcs will have a slightly different character. There is a constant voltage at the output of the capacitor filter rectifier circuit, and the circuit's load can be equivalent to a resistor. Figure 5 shows a schematic representation of the current and voltage signals under normal conditions and at ASC.
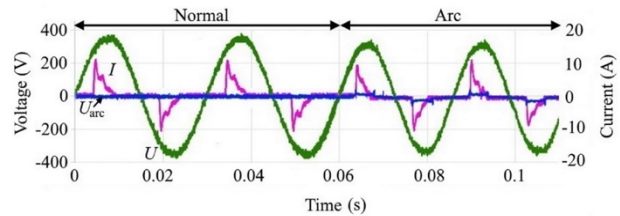

Fig. 5. Waveforms for current and voltage under normal conditions and when ASC occurs for a diode rectifier with a capacitor filter

With a rectifier circuit with a capacitive filter, under normal conditions, the voltage across the capacitor is lower than the voltage with the rectifier, then the capacitor is charged and the current is generated from the power source and an increase in the current in the circuit is observed. In the case of an increase in the voltage on the capacitor after charging, the capacitor is discharged to the rectifier load and the current near the source will be zero. Therefore, under normal conditions, a shoulder is observed on the current waveform for this type of load (Figure 5).

In addition, the arc voltage is zero. As one can see, when ASC occurs, as a rule, the voltage rise rate on the capacitor is higher than on the diode rectifier, which leads to sharp voltage drops across the arc, which is reflected in the nature of the current curve. In addition, the amplitude of the voltage at the source U and the amperage I also decrease due to energy dissipation in the load. When voltage rises U_{arc} ASC occurs and a current appears in the form of a pulse, and as a result, the diode turns on randomly. This is due to the uncertainty in the distance between the arc electrodes, which leads to uncertain changes U_{arc} [10].

To improve the current waveform, for these types of loads, an inductive filter (EMI) is added after the diode rectifier circuit to reduce the slope of the current while charging the capacitor [26]. Figure 6 shows the voltage and current waveforms under load from a diode rectifier with a capacitor filter circuit equipped with an EMI filter under various conditions.
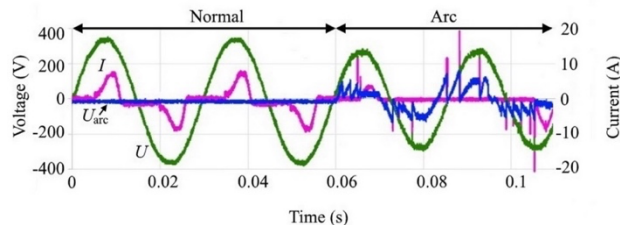

Fig. 6. Waveforms for current and voltage under normal conditions and when ASC occurs for a diode rectifier with a capacitor filter and an inductive EMI filter

Figure 6 shows that under normal conditions, due to the presence of inductance in the filter, there is no sharp change in the shape of the current curve I, but there are also shoulders with a longer shoulder length. In addition, the waveforms of

the current I in each half-cycle are approximately the same and there is no randomness. In the case where the voltage across the capacitor is less than that on the AC source, the arc resistance is very high and the current I is zero. When the value of the voltage on the capacitor U_{arc} is exceeded, the latter increases and the arc is ignited, but the diodes are blocked and I is equal to zero. In addition, the EMI inductance also blocks the passage of the current that goes to charge the capacitor. After charging it, there is a sharp increase in I, however, due to the small capacitance of the capacitor, the voltage U_{arc} drops faster than the voltage at the output U, as a result of which a sharp drop in current I and extinguishing of the arc occur.

In the case of a resistive-inductive type of load (for example, in an electric drill), an inductive circuit is connected to the circuit after the resistor. Figure 7 shows the waveform for this type of load.
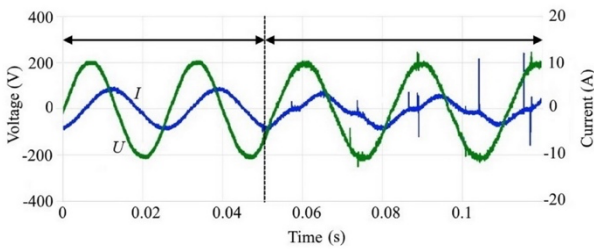

Fig. 7. Waveforms for current and voltage under normal conditions and when ASC occurs with resistive-inductive load

As seen under normal conditions, the VAC curves show no shoulder and momentum phenomena. When ASC occurs, shoulders and current pulses are observed. When the current passes through zero, the arc extinguishes and the voltage U will be almost the same as U_{arc}. The capacitor is charging, and while the ASC is taking place, the capacitor generates a pulse current. The pulses on the U voltage curve generate the inductance of the coil, which creates a voltage difference between the capacitor and U.

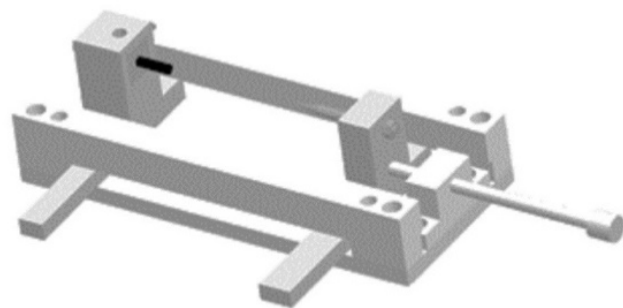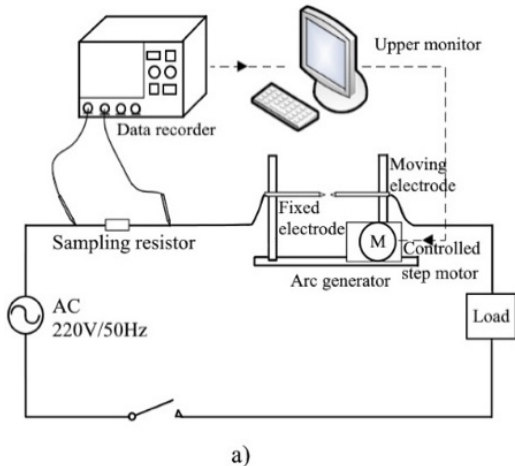Above is a brief description of the shoulder and impulse phenomena caused by ASC under various types of loads.

Depending on the type of load, VAC are very different, but there is a common feature, which is the randomness of the current waveform during ASC due to the uncertainty in the distance of the arc electrodes. According to Ohm's law for the entire circuit, when the waveform of the power supply voltage remains practically unchanged (the exception may be in amplitude), then the arc resistance changes continuously, which leads to significant changes in current. Analyzing current in the frequency domain will show high frequency noise components and random characteristics in the frequency domain.
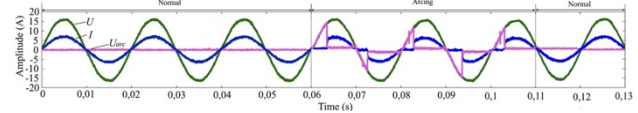

Fig, 8. Using Equation 1 for a purely resistive load with detection time in the signal

When the load S_n from equation (1) of the test circuit in Figure 8 is a purely resistive load, the voltage and current waveforms with each cell $i(t)_n$ will change over time when arcing current and voltage waveforms are generated. Figure 8. Shows the waveforms during the occurrence of a series arc fault and in the normal state. Since the impedance of a linear load is purely resistive, a series arc can also be equivalent to a resistance whose value undergoes dynamic changes, and thus forms the phase of arc formation. When the voltage and current are reduced to zero, the arc is extinguished. During this period the arc resistance is much greater than the load resistance, and U_{arc} is approximately equal to U. When the value increases to $U_{arc} = S_n$, the arc gap is broken and a series arc occurs. The voltage and current waveforms during the decay period are not much different from the period during which no arc occurs.

The arc detection time in Figure 8 was 0.6 seconds with a duration in the interval up to 0.11 seconds, after which the shape of the carrier signal returned to its previous state.

Fig. 9. Experimental setup (a) for determining and detecting sequential arc faults (SAF); (b) sequential arc fault generator\

3.2 Experimental measurement results and SAF detection

The samples are collected on the experimental setup, which is shown in Figure 9 and consists of a 220 V/50 Hz AC source, an arc generator, which consists of fixed and moving electrodes and an active load. In addition, the experimental setup includes a sampling resistor, a controlled motor and a monitor. Arc faults are generated by the DH-1 arc fault simulation generator designed according to UL1699.

Resistive, inductive, capacitive and switched load currents in normal and arc conditions are sampled at 25 kHz using the HIOKI 8860-50 data logger.

The stepper commutator motor provides a quick start and functions in stop and reversing modes. To activate the parallel arc fault condition in the system, the motor is subjected to a test procedure which consists in operating cycles of 1000 operating cycles with a frequency of two operating cycles per

1 minute in case the current is less than 25 A with a period of 1.5 to 2 s.

Figure 10 shows the results of measuring current signals at various loads, measured using the experimental setup. As can be seen from Figure 10, the characteristic changes of the curves in the arc state are observed to a greater extent in the electric drill and vacuum cleaner, which are characterized by a spectral distribution in time, the curve of the arc-shaped fluorescent lamp slightly differs from the normal waveform.

Operation time of protection at arc breakdown current of 2.5 A should not exceed 1 s; with increasing detected current operation time decreases consistently, up to 0.12 s at current of 32 A and above.
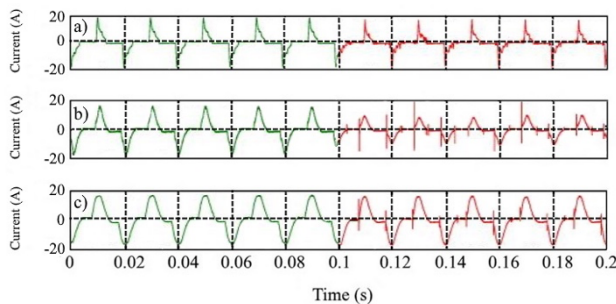
Fig. 10. Current signals under normal conditions (green line) and at SAF (red line) for various types of load in the network: fluorescent lamp (a), electric drill (b), and vacuum cleaner (c)

The Rigol MSO5074 oscilloscope is used as a data logger, whose sampling rate is equal to the rate at which the oscilloscope can digitize the input signal. At higher values it is responsible for high values of bandwidth of single signals, which gives a better resolution. The sampling rate value can be applied to a single channel, and when working with multiple channels simultaneously, the value of this characteristic decreases and can lead to the appearance of distorted signals. With the help of cursor measurement modes the amplitude and time measurements are performed by placing vertical or horizontal cursors at the desired points of the oscillogram.

As can be seen from Figure 10, the curves obtained from the experimental measurements are according to the theoretical description in the normal and arc state, where the loads of the vacuum cleaner and the electric drill slightly deviate from the normal values when the arc occurs. In addition, the off time of the system was recorded after more than 50 measurements, according to the proposed SAF method

A characteristic feature of the arc breakdown current is a wide spectrum with a frequency distribution that is close to pink noise and extends up to about 1 GHz. This broadband signal is naturally modulated by a doubled line frequency (100 or 120 Hz): in the vicinity of the line voltage transition through zero, where the arc is interrupted and the generation of high frequency interference stops; as the instantaneous voltage value increases, the arc ignites again.

Figure 11 shows the spectral distribution of three household appliances under arc and normal current conditions. Signs of an arc are evident in both the low- and high-frequency region. Under arc conditions, the low-frequency component in most appliances decreases and the high-frequency component increases. In the arc condition, the frequency of the inductive load (vacuum cleaner and power drill) has an irregular waveform, unlike that of a fluorescent lamp. The spectrum of the different types of load differs between each other in normal and arc states, which is explained by the presence of a switching load in the circuit, when in the normal state its current contains quite a few harmonic components.
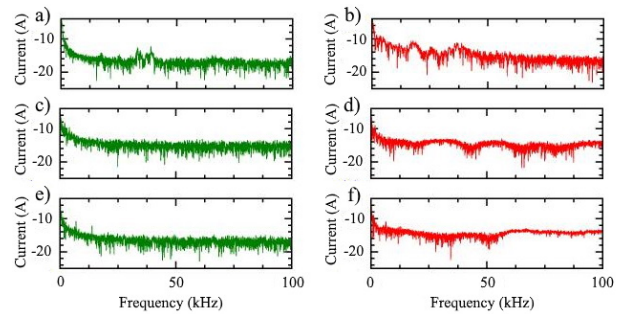
Fig. 11. Frequency spectrum distribution of current in normal and arc states. The graphs of (a) a fluorescent lamp (c) an electric drill (e) a vacuum cleaner represent the current waveform in the normal state; the graphs of (b) a fluorescent lamp (d) an electric drill (f) a vacuum cleaner represent the waveform in the arc state

During laboratory tests at ASC, a small current amplitude was observed (with an amplitude of up to 20 A) with a detection time of 0.15. The results obtained demonstrate good agreement with the results of other works, which confirms the correctness of the chosen method for detecting SAF proposed in this article. Thus, in [17], using the Fourier transforming method and training neural networks, it was found that SAF was recorded for various types of load during one half-period. Besides, studies of ASC for direct current in photovoltaic systems in [28] showed that noise for frequencies below 50 kHz increases, and frequency components below 5 kHz are more sensitive to changes in the width of the air gap.

This method of sequential arc fault detection is inferior to the discrete wavelet transform method, which is based on harmonic analysis. Detection of harmonic components contained in the standards is based on a fast Fourier transform for the amplitude-frequency spectrum, and the information associated with time is lost [29].

Further research may focus on load studies and methods for detecting sequential arc faults using discrete transformation and algebraic models.

4. Conclusion

This paper analyzed the use of volt-ampere characteristics for AC circuits under different loads of electrical appliances: fluorescent lamp, vacuum cleaner and electric drill.

The test procedure for currents less than 25 A was performed of 1000 duty cycles with a frequency of two duty cycles per minute and a period of 1.5 to 2 s.

The results of measurements of current signals under different load conditions showed that the characteristic curve changes under arc conditions have a dependence on the SAF and a spectral distribution in time with a frequency of 50 Hz and a wide spectrum with a frequency distribution. Under arc conditions the frequency of inductive load (vacuum cleaner and drill) showed an irregular waveform in contrast to the fluorescent lamp. The spectrum of different types of loads differs between each other in the normal and arc states, which is explained by the presence of a switched load in the circuit, the current of which in the normal state contains quite a lot of harmonic components.

In laboratory tests in SAF observed a small current amplitude of 15A at 220V, where the tripping time was 0.15s.

Further research can be aimed at studying the load and methods of detection of sequential arc faults using discrete transform and wavelet decomposition of signals.

_____

References

1. Federal State Budgetary Institution 'All-Russian Scientific Research Institute for Problems of Civil Defense and Emergencies of Russian Emergency Situations Ministry', Moscow (2021). https://www.mchs.gov.ru/dokumenty/5304
2. EFFIS Statistics, EFFIS - Estimates per Country, EFFIS (2020). https://effis.jrc.ec.europa.eu/apps/effis.statistics.portal/effis-estimates/EU
3. Underwriters Laboratories, UL 1699. UL Standard for Arc-Fault Circuit-Interrupters, 2nd ed., Underwriters Laboratories Inc., New York, NY, USA (2017).
4. International Electrotechnical Commission, General Requirements for Arc Fault Detection Devices; IEC 62606, International Electrotechnical Commission, Geneva, Switzerland (2017).
5. General Administration of Quality Supervision, Inspection and Quarantine of the People's Republic of China; Standardization Administration of the People's Republic of China, Electrical Fire Monitoring System–Part 4: Arcing Fault Detectors (GB14287.4-2014), Standards Press of China, Beijing, China (2014).
6. General Administration of Quality Supervision, Inspection and Quarantine of the People's Republic of China; Standardization Administration of the People's Republic of China, General Requirements for Arc Fault Detection Devices (AFDD) (GB/T 31143), Standards Press of China, Beijing, China (2014).
7. S. Kumar, B. S. Rajpurohit, S. N. Singh, I. Marinova and V. Mateev, 2020 21st National Power Systems Conf. (NPSC), IEEE, Gandhinagar, India, 2020, pp. 1–5 (2020).
8. N. El-Sherif, T. A. Domitrovich and F. P. Reyes, IEEE Ind. Appli. Mag. 27 (1), 55–68 (2020).
9. Y. Gao, L. Wang, Y. Zhang and Z. Yin, 2019 Prognostics and System Health Management Conf. (PHM-Qingdao), IEEE, Qingdao, China, pp. 1–5 (2019).
10. [K. Zeng, L. Xing, Y. Zhang and L. Wang, 2017 Prognostics and System Health Management Conf. (PHM-Harbin), IEEE, Harbin, China, pp. 1–5 (2017).
11. K. Yang, R. Chu, R. Zhang, J. Xiao and R. Tu, Sensors 20 (1), Art no. 162 (2020).
12. M. Atharparvez and K. R. Purandare, 2018 IEEE Holm Conf. Electrical Contacts, IEEE, Albuquerque, NM, USA, pp. 335–339 (2018).
13. L. Kang, J. Zhang, H. Zhou, Z. Zhao and X. Duan, Electronics 10 (4), Art no. 426 (2021).
14. E. Tisserand, J. Lezama, P. Schweitzer and Y. Berviller, Electr. Power Syst. Res. 119, 91–99 (2015).
15. R. Chu, P. Schweitzer and R. Zhang, Sensors 20 (17), Art no. 4910 (2020).
16. L. Chong and L. Jiahong, Electr. Eng. 12, 1–7 (2017).
17. M. A. Abdulrachman, E. Prasetyono, D. O. Anggriawan and A. Tjahjono, 2019 Int. Electronics Symposium (IES), IEEE, Surabaya, Indonesia, pp. 439–445 (2019).
18. W. Liu, X. Zhang, Y. Dong and X. Huang, IECON 2017-43rd Ann. Conf. IEEE Industrial Electronics Society, IEEE, Beijing, China, pp. 4104–4109 (2017).
19. A. Sawicki and M. Haltof, Arch. Electr. Eng. 65 (1), 87–103 (2016).
20. A. F. Ilman, 2018 Int. Conf. Applied Engineering (ICAE), IEEE, Batam, Indonesia, pp. 1–5 (2018).
21. Y. Wang, F. Zhang, X. Zhang and S. Zhang, IEEE Trans. Indust. Inform. 15 (12), 6210–6219 (2018).
22. D. Giordano, D. Signorino, D. Gallo, H. E. van den Brom and M. Sira, Sensors, 20 (23), Art no. 6935 (2020).
23. H. Gao, Z. Wang, A. Tang, C. Han, F. Guo and B. Li, IEEE Trans. Instrum. Meas. 70, 1–8 (2021).
24. J. E. Siegel, S. Pratt, Y. Sun and S. E. Sarma, Eng. Appl. Artif. Intell. 74, 35–42 (2018).
25. L. N. Bagautdinova, R. S. Sadriev, A. F. Gaysin, R. T. Nasibullin, F. M. Gaysin and S. C. Mastyukov, High Temp. 58 (3), 441–443 (2020).
26. S. Kuehnel, S. Kornhuber and J. Lambrecht, 2018 IEEE Conf. Electrical Insulation and Dielectric Phenomena (CEIDP), IEEE, Cancun, Mexico, pp. 313–317 (2018).
27. Q. Lu, Z. Ye, Y. Zhang, T. Wang and Z. Gao, Energies 12 (2), Art no. 323 (2019).
28. GOST, GOST IEC 62606-2016. *Arc fault detection devices for household and similar use.* General requirements. Interstate classifier of standards 29.120.50 (2018).
29. S. Zhi-ting, Y. Lu and H. Di, 2018 13th World Congress on Intelligent Control and Automation (WCICA), IEEE, pp. 1026–1030 (2018).
30. V. Apetrei, C. Filote and A. Graur, Ninth Int. Conf. Ecological Vehicles and Renewable Energies (EVER), Monte-Carlo, Monaco, pp. 1–8 (2014).